

Statistical Mechanics of Broadcast Channels Using Low Density Parity Check Codes

Kazutaka Nakamura* and Yoshiyuki Kabashima†

*Department of Computational Intelligence and Systems Science,
Tokyo Institute of Technology, Yokohama 226-8502, Japan*

Robert Morelos Zaragoza‡

*Advanced Telecommunication Laboratory,
SONY Computer Science Laboratories, Inc.,
Shinagawa, Tokyo 141-0022, Japan*

David Saad§

*The Neural Computing Research Group, School of Engineering
and Applied Science, Aston University, Birmingham B4 7ET, UK
(Dated: December 9, 2002)*

We investigate the use of Gallager's low-density parity-check (LDPC) codes in a degraded broadcast channel, one of the fundamental models in network information theory. Combining linear codes is a standard technique in practical network communication schemes and is known to provide better performance than simple time sharing methods when algebraic codes are used. The statistical physics based analysis shows that the practical performance of the suggested method, achieved by employing the belief propagation algorithm, is superior to that of LDPC based time sharing codes while the best performance, when received transmissions are optimally decoded, is bounded by the time sharing limit.

PACS numbers: 89.70.+c, 75.10.Hk, 05.50.+q, 05.70.Fh, 89.70.+c

I. INTRODUCTION

Progress in digital communication technologies has dramatically increased the information flow in both wired and wireless channels. This makes the role of generic coding techniques, such as error-correcting codes and data compression, more important. As most existing codes are constructed for simple point-to-point communication, they do not necessarily provide optimal performance in multi-terminal communication such as the inter-net, mobile phones and satellite communication. Therefore, designing improved codes that utilize characteristic properties of these media is a promising direction for enhancing the performance of multi-terminal communication.

The broadcast channel is a standard multi-terminal communication channel composed of a single sender and multiple receivers, and is characteristic of TV and radio broadcasting. Unlike point-to-point communication, the sender (TV station) simultaneously broadcasts multiple messages (TV programs) to many receivers (TV sets) simultaneously via noisy channels. This implies that constructing a jointly optimal code with respect to the multiple channels may provide improved performance (i.e., higher capacity) than that of the time sharing scheme, whereby separate optimally designed code are used for each channel. Actually, Cover showed that jointly op-

timized codes can have a larger capacity region, where error free communication becomes possible, than that of time sharing codes, in *degraded channels* which are one of representative models of broadcast communication [1–4]. However, his proof is non-constructive and the search for better practical codes for broadcast channels is still an important topic in information theory (IT).

The purpose of this paper is to devise and analyze an improved practical code for a degraded broadcast channel by linearly combining Low-Density Parity-Check (LDPC) codes, which have been shown to provide nearly optimal performance for single channels [5–7]. For Reed-Solomon and BCH codes, which are standard suboptimal codes, it has been reported that combining codes linearly results in superior performance with respect to a time shared transmission [8, 9]. This provides the motivation for the current study, investigating the performance of linearly combined LDPC codes.

Generally, one can define two different performance measures for evaluating LDPC codes. The first is the *practical* performance achievable in feasible time scales that grow polynomially with the systems size; while the other is the *optimal* theoretically achievable performance, for which the required computation typically increases exponentially with respect to the message length. Utilizing the similarity between LDPC codes and Ising spin systems, statistical physics provides a scheme for evaluating both performance measures within the same framework [10–12]; the current standard method used in the information theory community [13] can only provide an estimate of the practical performance, and practically reduces to the one used within the statistical physics frame-

*Electronic address: knakamur@fe.dis.titech.ac.jp

†Electronic address: kaba@dis.titech.ac.jp

‡Electronic address: morelos@csl.sony.co.jp

§Electronic address: d.saad@aston.ac.uk

work. In this paper, we show that the statistical physics based analysis points to a superior practical performance of the suggested method with respect to LDPC based time sharing codes (achieved by employing the belief propagation algorithm); while its optimal performance is bounded by the timesharing limit, which cannot be saturated by known practical methods.

This paper is organized as follows. In the next section, we introduce the general framework for broadcast channels. Unlike simple communication channels, the optimal communication performance is still unknown for most broadcast channels, which would make it difficult to evaluate the performance of the proposed scheme. Therefore, we focus here on the degraded channel, for which the capacity region has already been obtained. In section III, an LDPC code based construction for degraded channels is introduced, and is subsequently analyzed in section IV using methods of statistical physics. In section V, the performance of the proposed scheme is evaluated by solving numerically equations that emerge from the analysis. The final section is devoted to a summary and conclusion.

II. DEGRADED BROADCAST CHANNEL

In the general framework of broadcast channels, a single sender (station) broadcasts a codeword composed of different messages to multiple receivers. For simplicity, we here restrict our attention to the case of two receivers (Fig. 1), where one codeword \mathcal{X} (N bits), comprising two messages \mathcal{W}_1 ($R_1 N$ bits) and \mathcal{W}_2 ($R_2 N$ bits), is sent to two receivers. As each channel is noisy, receivers 1 and 2 obtain two corrupted codewords \mathcal{Y}_1 and \mathcal{Y}_2 , respectively; this is modeled by a conditional probability $P(\mathcal{Y}_1, \mathcal{Y}_2 | \mathcal{X})$. The received corrupted codewords \mathcal{Y}_1 and \mathcal{Y}_2 are decoded by the respective receivers to retrieve only the message addressed to each of them.

Analogously to the case of single channels, error free communication becomes possible if the corresponding code rate vector (R_1, R_2) lies within a certain convex region, termed the *capacity region*, determined for a given broadcast channel $P(\mathcal{Y}_1, \mathcal{Y}_2 | \mathcal{X})$ using an infinite code length N [3]. Evaluation of the capacity region is one of the fundamental problems in information theory; the problem is generally difficult and has not yet been solved in general except for a few special cases.

A broadcast channel $P(\mathcal{Y}_1, \mathcal{Y}_2 | \mathcal{X})$ is termed *degraded* if there exists a distribution $P'(\mathcal{Y}_2 | \mathcal{Y}_1)$ such that

$$P(\mathcal{Y}_2 | \mathcal{X}) = \sum_{\{\mathcal{Y}_1\}} P'(\mathcal{Y}_2 | \mathcal{Y}_1) P(\mathcal{Y}_1 | \mathcal{X}). \quad (1)$$

This channel model can be used for representing a situation that the rate of noise corruption becomes higher as a receiver is located in a farther distance from a broadcast station (sender), which is a natural assumption for both of wired and wireless communication. Assuming

that the corruption rate only depends on the communication distance, which is also natural at least as a first approximation, the channel model in the farther distance ($P(\mathcal{Y}_2 | \mathcal{X})$) can be *formally* expressed as if the message were conveyed via the receiver in the closer distance in a relay scheme (eq. (1)) although the two receivers does not communicate with each other actually (Fig. 1. (c)).

The degraded channel is exceptional in the sense that its capacity region can be analytically obtained as the convex hull of the closure of all points (R_1, R_2) that satisfy

$$\begin{cases} R_2 < I(\mathcal{U}; \mathcal{Y}_2) \\ R_1 < I(\mathcal{X}; \mathcal{Y}_1 | \mathcal{U}) \end{cases} \quad (2)$$

for a certain joint distribution $P(\mathcal{U})P(\mathcal{X} | \mathcal{U})P(\mathcal{Y}_1, \mathcal{Y}_2 | \mathcal{X})$; where the auxiliary random variable \mathcal{U} has a cardinality bounded by $|\mathcal{U}| \leq \min\{|\mathcal{X}|, |\mathcal{Y}_1|, |\mathcal{Y}_2|\}$. This region is often called Cover's capacity [1] region. Unfortunately, the derivation of Cover's capacity is non-constructive and offers little clue to design efficient practical codes. Thus, practical codes for the degraded broadcast channel has been actively investigated in the network information theory [4].

In the case of binary symmetric channels characterized by flip probabilities p_1 and p_2 , condition (1) reduces to an inequality $p_2 > p_1$. Then, the expression of Cover's capacity is simplified to

$$\begin{cases} R_2 < 1 - H_2(\delta * p_2) \\ R_1 < H_2(\delta * p_1) - H_2(p_1) \end{cases} \quad (3)$$

where a parameter $0 < \delta < 1$ specifies the optimal ratio between R_1 and R_2 ; $\delta * p = \delta(1-p) + (1-\delta)p$ and $H_2(p)$ is Shannon's entropy $H_2(p) = -p \log_2 p - (1-p) \log_2 (1-p)$.

The solid convex curve in Fig.1(b) shows Cover's limit, i.e., the boundary of Cover's capacity for the binary symmetric channels. The straight broken line corresponds to the timesharing capacity, i.e., the achievable capacity by concatenating two independent codeswords optimized for each channel separately. This is realized by using $N(1-\alpha)$ and $N\alpha$ bits of codeword \mathcal{X} for encoding messages \mathcal{W}_1 and \mathcal{W}_2 , respectively. Here, $0 < \alpha < 1$ is the code length ratio between the two messages. This simple concatenation and the limit achievable by this scheme are often termed the *timesharing* and the *timesharing limit*, respectively. The difference between Cover's and the timesharing limits indicates the capacity gain obtained by optimizing a code for the complete broadcasting system in comparison with respect to optimizing each of the channels separately.

We have to emphasize that achieving the timesharing limit *in practice* is never trivial as there is no known practical code that saturates Shannon's limit even for a single channel. Therefore, the design of improved practical codes for broadcasting, by combining existing codes, devised for single channels, is an important research topic in coding theory [4].

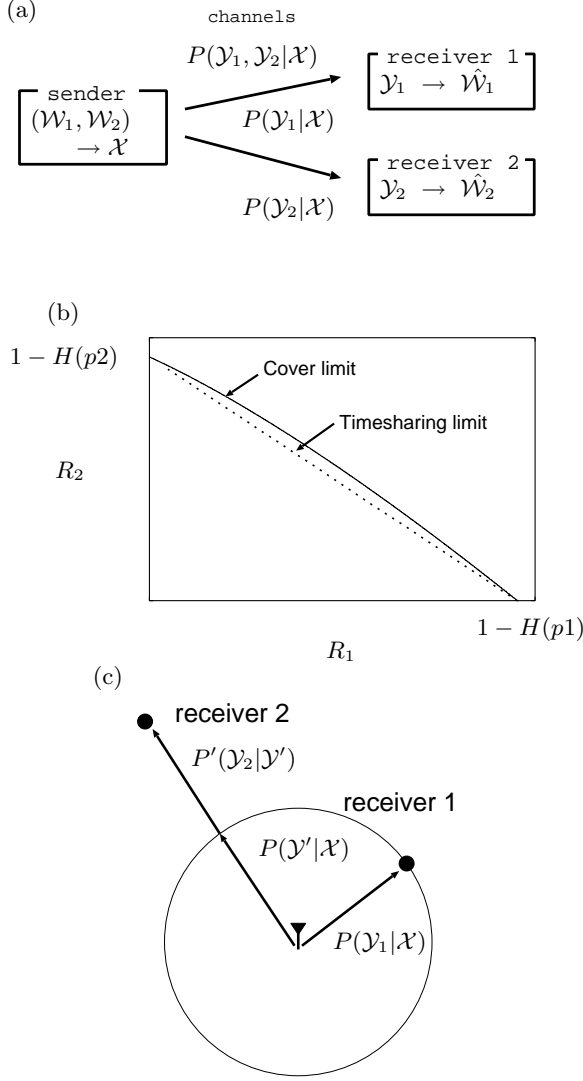


FIG. 1: (a): A single sender and two receivers broadcast channel. (b): The capacity region in the case of binary symmetric channels. The solid curve and the dotted line denote Cover's and timesharing limits, respectively. (c): When the corruption rate increases proportional to the distance from a broadcast station (sender), the functional form of the conditional probability $P(\mathcal{Y}|\mathcal{X})$ becomes identical on a circular arc of a fixed radius centred at the station. This implies that the conditional probability for the second receiver can be expressed as $P(\mathcal{Y}_2|\mathcal{X}) = \sum_{\mathcal{Y}'} P(\mathcal{Y}_2|\mathcal{Y}')P(\mathcal{Y}'|\mathcal{X}) = \sum_{\mathcal{Y}_1} P(\mathcal{Y}_2|\mathcal{Y}_1)P(\mathcal{Y}_1|\mathcal{X})$, where \mathcal{Y}' is the received codeword at the closest point to the second receiver on the circular arc, as if the codeword were conveyed to the second receiver in a relay scheme via the first receiver.

III. LINEARLY COMBINED CODES

Linearly combined codes is a well-known strategy for designing high performance communication schemes

for broadcast channels using multiple linear Error-Correcting Codes (ECC) [8, 9]. In this scheme, the first $N(1 - \alpha)$ bits of a codeword are obtained by linearly mixing two messages \mathcal{W}_1 and \mathcal{W}_2 while the other $N\alpha$ bits are generated only from \mathcal{W}_2 by some linear transformation. In both coding and decoding, all operations are typically carried out in modulo 2. This method has been developed for algebraic codes, such as Reed-Solomon and BCH, which are standard codes designed for relatively short code lengths. For these codes, it is reported that the minimum distance between codewords is larger than that achieved in the timesharing scheme, which implies higher robustness against channel noise [8, 9].

However, it is unclear whether a similar construction also offers better performance when different code types are used. Furthermore, it is theoretically interesting and important to examine whether a linearly combined code can saturates Cover's limit for infinite code length (N) or not.

Motivated by these questions, we investigate here the ability and limitations of linearly combined LDPC codes in the limit $N \rightarrow \infty$.

An LDPC code is characterized by a parity check matrix. To devise a linearly combined coding scheme for LDPC codes, we define a parity check matrix in an upper triangular form

$$A = \begin{pmatrix} A_1 & A_2 \\ 0 & A_3 \end{pmatrix} \quad (4)$$

where the sizes of the sub-matrices A_1, A_2, A_3 are $[(1 - \alpha)N - R_1N] \times (1 - \alpha)N$, $[(1 - \alpha)N - R_1N] \times \alpha N$, $[\alpha N - R_2N] \times \alpha N$, respectively. Further, we assume that A_1, A_2, A_3 have K_1, K_2, K_3 and C_1, C_2, C_3 non-zero elements per row and column, respectively. Based on the parity check matrix, the generator matrix G^T is constructed as

$$G^T = \begin{pmatrix} G_1^T & G_2^T \\ 0 & G_3^T \end{pmatrix} \quad (5)$$

where G_i^T ($i = 1, 3$) are constructed systematically to satisfy the constraints $A_i G_i^T = 0 \pmod{2}$ and G_2^T is defined as $-A_1^T [A_1 A_1^T]^{-1} [A_2 G_3^T]$. The sizes of these matrices are $(1 - \alpha)N \times R_1N$, $\alpha N \times R_2N$ and $\alpha N \times R_2N$, respectively.

The sender produces a codeword \mathcal{X} by taking a product of the generator matrix G^T and the original messages $(\mathcal{W}_1, \mathcal{W}_2)^T$. Receiving a possibly corrupted codeword, each receiver evaluates the syndrome vectors $\mathbf{J}_i = A\mathcal{Y}_i$ ($i = 1, 2$), which yield the parity-check equation $\mathbf{J}_i = A\xi_i$. The message vector ξ_i can be thought of as having two separate segments denoted by \mathbf{u} (up) and \mathbf{d} (down) later on. The parameter α controls the error correction ability for the second message; the transmitted information redundancy increases with α . The decoding problem for each receiver is to find the most probable messages, \mathbf{s}_i and σ_i , such that the parity check equation

$$\mathbf{J}_i = \begin{pmatrix} A_1 & A_2 \\ 0 & A_3 \end{pmatrix} \begin{pmatrix} \mathbf{s}_i \\ \sigma_i \end{pmatrix} \quad (i = 1, 2) \quad (6)$$

is obeyed, and using prior knowledge about the two noise vectors characterized by the two different channels.

The second receiver has to estimate only the lower part of noise vector ξ^d , which can be carried out using only the lower part of Eq.(6). However, we assume here that both receivers independently solve Eq.(6) using prior knowledge on their own channels since one can show that solving the whole equation provides the optimal estimation performance for both receivers. As Eq.(6) has the same form for receivers 1 and 2, we hereafter omit the subscript $i = 1, 2$.

It might be emphasized here that the upper triangular architecture in the parity check matrix A is suitable for providing a higher error correction ability to the second message \mathcal{W}_2 which is, probably, more degraded according to Eq. (1) than the other message \mathcal{W}_1 as ξ^d can be estimated independently of ξ^u while estimation of ξ^u fails unless ξ^d is correctly retrieved. Later, this property of the current code, in conjunction with assignment of sufficient resource to \mathcal{W}_2 in code construction, will show a seemingly counter-intuitive feature in performance.

For bit-wise minimization of the error probability the optimal estimation is given by maximizing the posterior marginal (MPM)

$$\hat{\xi}_i^u = \operatorname{argmax}_{s_i \in \{0/1\}} P(s_i | \mathbf{J}), \quad \hat{\xi}_j^d = \operatorname{argmax}_{\sigma_j \in \{0/1\}} P(\sigma_j | \mathbf{J}). \quad (7)$$

An exact evaluation of Eq.(7) is generally hard; therefore, the belief propagation (BP) approximation scheme is widely used as a practical decoding algorithm. The latter has been shown to be identical to the Thouless-Anderson-Palmer (TAP) approach in the current case [14, 17, 18].

IV. STATISTICAL MECHANICS

A. Macroscopic analysis – performance evaluation

In order to evaluate the typical error-correction ability of these codes in the limit $N \rightarrow \infty$, we investigate the behavior of the MPM decoder using the established methods of statistical mechanics. We first map the current system to an Ising spin model with finite connectivity, by employing the binary representation $\{+1, -1, \times\}$ for the alphabet and operator instead of the Boolean one $\{0, 1, +\}$. This implies that the posterior probability $P(\mathbf{s}, \boldsymbol{\sigma} | \mathbf{J})$ can be expressed as a Boltzmann distribution at the inverse temperature $\beta = 1$ using a Hamiltonian

$$\begin{aligned} \mathcal{H}(\mathbf{s}, \boldsymbol{\sigma} | \mathbf{J}) = \lim_{\gamma \rightarrow \infty} & \left\{ \gamma \sum_{\{\mathcal{I}(K_1), \mathcal{J}(K_2)\}} D_{\mathcal{I}(K_1), \mathcal{J}(K_2)}^{1,2} \delta(-J_{\mathcal{I}(K_1), \mathcal{J}(K_2)}^u; \prod_{i \in \mathcal{I}(K_1)} s_i \prod_{j \in \mathcal{J}(K_2)} \sigma_j) \right. \\ & \left. + \gamma \sum_{\{\mathcal{J}(K_3)\}} D_{\mathcal{J}(K_3)}^3 \delta(-J_{\mathcal{J}(K_3)}^d; \prod_{j \in \mathcal{J}(K_3)} \sigma_j) \right\} - F \sum_{i=1}^{(1-\alpha)N} s_i - F \sum_{j=1}^{\alpha N} \sigma_j, \end{aligned} \quad (8)$$

where $\mathcal{I}(K) = \langle i_1, i_2, \dots, i_K \rangle$ denotes the combination of the K subscripts chosen from the $i = 1, 2, \dots, (1 - \alpha)N$ possibilities without duplication (the order is ignored), and $\mathcal{J}(K) = \langle j_1, j_2, \dots, j_K \rangle$ is the K combination from $j = 1, 2, \dots, \alpha N$ chosen similarly. The tensor $D_{\mathcal{I}(K_1), \mathcal{J}(K_2)}^{1,2}$ becomes 1 when its subscripts agree with the positions of non-zero elements in the parity-check matrices A_1 and A_2 , and 0 otherwise. The tensor $D_{\mathcal{J}(K_3)}^3$ similarly corresponds to A_3 . The first and second terms in Hamiltonian (8) correspond to Eq.(6) while the third and fourth terms are provided by the prior distribution of the noise. The field F represents the channel noise level; it is set to $\frac{1}{2} \ln(1 - p_1)/p_1$ and $\frac{1}{2} \ln(1 - p_2)/p_2$ for the first and the second receivers, respectively.

In order to simplify the calculation, we first employ the gauge transformation $s_i \rightarrow s_i \xi_i^u, \sigma_j \rightarrow \sigma_j \xi_j^d, J_{\dots}^u \rightarrow 1$ and $J_{\dots}^d \rightarrow 1$, which reduces complicated couplings expressed in the first and second terms in Hamiltonian (8)

to simple ferromagnetic interactions.

As the parity check matrices and noise vectors are generated randomly, we have to perform averages over these variables for extracting typical properties of the code. This can be carried out by the replica method $-\beta \mathcal{F} = \langle \ln \mathcal{Z} \rangle_{A, \xi^u, \xi^d} = \lim_{n \rightarrow 0} (1/n) \ln \langle \mathcal{Z}^n - 1 \rangle_{A, \xi^u, \xi^d}$, where \mathcal{Z} is the partition function and $\langle \dots \rangle_{A, \xi^u, \xi^d}$ represents an average over the parity check matrix A and the noise vectors ξ^u and ξ^d (i.e., the quenched variables).

This gives rise to three sets of order parameters

$$\begin{aligned} q_{\{a_1, a_2, \dots, a_m\}} &= \frac{1}{N} \sum_{i=1}^{(1-\alpha)N} X_i s_i^{a_1} \dots s_i^{a_m}, \\ r_{\{a_1, a_2, \dots, a_m\}} &= \frac{1}{N} \sum_{j=1}^{\alpha N} Y_j \sigma_j^{a_1} \dots \sigma_j^{a_m}, \\ t_{\{a_1, a_2, \dots, a_m\}} &= \frac{1}{N} \sum_{j=1}^{\alpha N} Z_j \sigma_j^{a_1} \dots \sigma_j^{a_m} \end{aligned} \quad (9)$$

where a_1, a_2, \dots, a_m denote the replica indices running from 1 to n , and their conjugates $\hat{q}_{\{a_1, a_2, \dots, a_m\}}$, $\hat{r}_{\{a_1, a_2, \dots, a_m\}}$, $\hat{t}_{\{a_1, a_2, \dots, a_m\}}$. The variables Z_j are introduced to express the constraint of the parity-check matrix A_3 as

$$\begin{aligned} \delta \left(\sum_{\mathcal{J}(K_3) \setminus j} D_{\mathcal{J}(K_3)}^3 - C_3 \right) \\ = \oint \frac{dZ_j}{2\pi} Z_j^{\sum_{\mathcal{J}(K_3) \setminus j} D_{\mathcal{J}(K_3)}^3 - (C_3 + 1)}. \end{aligned} \quad (10)$$

The variables X_i and Y_j are similarly introduced for A_2 and A_3 .

In order to proceed further, one has to make an assumption about the symmetry of replica indices. Here we employ the simplest replica symmetric (RS) ansatz, expressed in the current case by $q_{\{a_1, \dots, a_m\}} = q_0 \int dx \pi(x) x^m$, $r_{\{a_1, \dots, a_m\}} = r_0 \int dy \rho(y) y^m$, $t_{\{a_1, \dots, a_m\}} = t_0 \int dz \phi(z) z^m$, where q_0 , r_0 and t_0 are the normalization constants to make $\pi(x)$, $\rho(y)$ and $\phi(z)$ proper probability distributions over the interval $[-1, 1]$, respectively. Unspecified integrals are performed over $[-1, 1]$. We also assume a similar ansatz for the conjugate variables. A further complicated assumption about the order parameter symmetry is generally required in most disordered systems [20, 21]. However, the validity of the RS ansatz in the current system is strongly supported by a recent report on the absence of the replica symmetry breaking in gauged systems where Nishimori's temperature is used [22]. The latter corresponds to using the correct priors in decoding [23], as performed in the current analysis.

Under these assumptions, one obtains the free-energy

$$\begin{aligned} \mathcal{F} &= (1 - R_1 - R_2) \ln 2 - (1 - \alpha - R_1) \left\langle \ln \left(1 + \prod_{l=1}^{K_1} x_l \prod_{l'=1}^{K_2} y_{l'} \right) \right\rangle_{\pi^{K_1}, \rho^{K_2}} - (\alpha - R_2) \left\langle \ln \left(1 + \prod_{l=1}^{K_3} z_l \right) \right\rangle_{\phi^{K_3}} \\ &+ (1 - \alpha) C_1 \left\langle \ln(1 + x\hat{x}) \right\rangle_{\pi, \hat{\pi}} + \alpha C_2 \left\langle \ln(1 + y\hat{y}) \right\rangle_{\rho, \hat{\rho}} + \alpha C_3 \left\langle \ln(1 + z\hat{z}) \right\rangle_{\phi, \hat{\phi}} \\ &+ (1 - \alpha) \left\langle \ln \left[\text{Tr}_s e^{s\xi^u F} \prod_{l=1}^{C_1} (1 + s\hat{x}_l) \right] \right\rangle_{\xi, \hat{\pi}^{C_1}} + \alpha \left\langle \ln \left[\text{Tr}_\sigma e^{\sigma\xi^d F} \prod_{l=1}^{C_2} (1 + \sigma\hat{y}_l) \prod_{l'=1}^{C_3} (1 + \sigma\hat{z}_{l'}) \right] \right\rangle_{\xi, \hat{\rho}^{C_2}, \hat{\phi}^{C_3}} \end{aligned} \quad (11)$$

where $\langle \dots \rangle_{PK}$ denotes an integral of the form $\int \prod_{k=1}^K dx_k P(x_k) (\dots)$ and $\langle f(\xi) \rangle_\xi = (1 - p)f(+1) + pf(-1)$.

Varying Eq.(11), one obtains a set of saddle-point equations,

$$\begin{aligned} \pi(x) &= \left\langle \delta \left(x - \tanh \left[\sum_{l=1}^{C_1-1} \tanh^{-1} \hat{x}_l + \xi^u F \right] \right) \right\rangle_{\xi, \hat{\pi}^{C_1-1}}, \\ \rho(y) &= \left\langle \delta \left(y - \tanh \left[\sum_{l=1}^{C_2-1} \tanh^{-1} \hat{y}_l \right. \right. \right. \\ &\quad \left. \left. \left. + \sum_{l'=1}^{C_3} \tanh^{-1} \hat{z}_{l'} + \xi^d F \right] \right) \right\rangle_{\xi, \hat{\rho}^{C_2-1}, \hat{\phi}^{C_3}}, \\ \phi(z) &= \left\langle \delta \left(z - \tanh \left[\sum_{l=1}^{C_2} \tanh^{-1} \hat{y}_l \right. \right. \right. \\ &\quad \left. \left. \left. + \sum_{l'=1}^{C_3-1} \tanh^{-1} \hat{z}_{l'} + \xi^d F \right] \right) \right\rangle_{\xi, \hat{\rho}^{C_2}, \hat{\phi}^{C_3-1}}, \end{aligned}$$

$$\begin{aligned}
\hat{\pi}(x) &= \left\langle \delta \left(\hat{x} - \prod_{l=1}^{K_1-1} x_l \prod_{l'=1}^{K_2} y_{l'} \right) \right\rangle_{\pi^{K_1-1}, \rho^{K_2}}, \\
\hat{\rho}(y) &= \left\langle \delta \left(\hat{y} - \prod_{l=1}^{K_1} x_l \prod_{l'=1}^{K_2-1} y_{l'} \right) \right\rangle_{\pi^{K_1}, \rho^{K_2-1}}, \\
\hat{\phi}(z) &= \left\langle \delta \left(\hat{z} - \prod_{l=1}^{K_3-1} z_l \right) \right\rangle_{\phi^{K_3-1}}
\end{aligned} \tag{12}$$

The overlaps $M_{\mathbf{u}} = \frac{1}{(1-\alpha)N} \sum_i \hat{s}_i \xi_i^{\mathbf{u}}$ and $M_{\mathbf{d}} = \frac{1}{\alpha N} \sum_j \hat{\sigma}_j \xi_j^{\mathbf{d}}$ serve as performance measures for the error-correcting ability. After solving the saddle-point equations (12) these can be calculated as

$$M_{\mathbf{u}} = \int dh h_{\text{eff}}^{\mathbf{u}}(h) \text{sign}(h), \quad M_{\mathbf{d}} = \int dh h_{\text{eff}}^{\mathbf{d}}(h) \text{sign}(h), \tag{13}$$

where distributions of effective fields $h_{\text{eff}}(h)$ are evaluated as

$$\begin{aligned}
h_{\text{eff}}^{\mathbf{u}}(h) &= \left\langle \delta \left(h - \tanh \left[\sum_{l=1}^{C_1} \tanh^{-1} \hat{x}_l + \xi F \right] \right) \right\rangle_{\xi, \hat{\pi}^{C_1}} \\
h_{\text{eff}}^{\mathbf{d}}(h) &= \left\langle \delta \left(h - \tanh \left[\sum_{l=1}^{C_2} \tanh^{-1} \hat{y}_l, \right. \right. \right. \\
&\quad \left. \left. \left. + \sum_{l'=1}^{C_3} \tanh^{-1} \hat{z}_{l'} + \xi F \right] \right) \right\rangle_{\xi, \hat{\rho}^{C_2}, \hat{\phi}^{C_3}}. \tag{14}
\end{aligned}$$

B. Microscopic analysis – practical decoding

As already mentioned, it is computationally hard to perform MPM decoding (7) exactly. Instead, the belief propagation (BP) algorithm [14] is widely used for a practical decoding in LDPC codes. Belief propagation has recently been shown to be equivalent to the Bethe method [15, 16] in general and to provide the Thouless-Anderson-Palmer (TAP) approach [17], in particular, for spin glass models [18, 19]. Since the current system is somewhat similar to spin glass models, we use a term *BP/TAP* for referring to this scheme from now on.

The BP/TAP approach offers an iterative algorithm to approximately evaluate marginal posterior distributions based on local dependencies between syndrome and variables. These local dependencies can be uniquely identified with conditional probabilities. In the current system, these become: $q_{\mu l}^n = P(n_l = n | \{\mathbf{J} \setminus J_{\mu}\})$ and $\hat{q}_{\mu l}^n \propto P(J_{\mu} | n_l = n, \{\mathbf{J} \setminus J_{\mu}\})$ where n_l and J_{μ} represent components of spin variables \mathbf{s} , $\boldsymbol{\sigma}$ and syndrome \mathbf{J} , respectively; $\{\mathbf{J} \setminus J_{\mu}\}$ denotes the set of syndrome bits excluding μ -th component. As most syndrome and spin variables are not directly related, we assign the conditional probabilities only to pairs μl that have non-zero elements in the parity check matrix A .

Evaluating the two types of conditional probabilities using directly connected components, the BP/TAP algorithm can be generally expressed as

$$q_{\mu l}^n = \alpha_{\mu l} e^{F n} \prod_{\nu \in \mathcal{M}(l) \setminus \mu} \hat{q}_{\nu l}^n, \tag{15}$$

$$\hat{q}_{\mu l}^n = \hat{\alpha}_{\mu l} \sum_{n_j \in \mathcal{L}(\mu) \setminus l} \delta(J_{\mu}; n \prod_{j \in \mathcal{L}(\mu) \setminus j} n_j) \prod_{j \in \mathcal{L}(\mu) \setminus l} q_{\mu j}^{n_j}, \tag{16}$$

where $\mathcal{M}(l)$ and $\mathcal{L}(\mu)$ denote the sets of syndrome and spin variable indices that are directly linked to spin and syndrome indices l and μ , respectively; $\mathcal{M}(l) \setminus \mu$ represents the set of indices $\nu \in \mathcal{M}(l)$ excluding μ and similarly for $\mathcal{L}(\mu) \setminus l$ and other sets. Normalization constants, $\alpha_{\mu l}$ and $\hat{\alpha}_{\mu l}$, are introduced to make $q_{\mu l}^n$ and $\hat{q}_{\mu l}^n$ probability distributions of spin variable n . A field F is introduced to represent the prior probability.

Since spin variable n takes only two values ± 1 , it is convenient to express the BP/TAP algorithm using spin averages $\sum_{n=\pm 1} n q_{\mu l}^n$ and $\sum_{n=\pm 1} n \hat{q}_{\mu l}^n$ rather than the distributions $q_{\mu l}^n$ and $\hat{q}_{\mu l}^n$ themselves. As the parity check matrix A is structured, it may be useful to assign different notation to the spin averages according to the submatrix to which the pair of indices μl belongs to. We use $x_{\mu l}$, $y_{\mu l}$ and $z_{\mu l}$ to denote $\sum_{n=\pm 1} n q_{\mu l}^n$ when the pair of indices μl belongs to A_1 , A_2 and A_3 , respectively. Similar notations $\hat{x}_{\mu l}$, $\hat{y}_{\mu l}$ and $\hat{z}_{\mu l}$ are used for $\sum_{n=\pm 1} n \hat{q}_{\mu l}^n$. Then, the BP/TAP algorithm (15) and (16), which is expressed as a set of functional equations, is reduced to a couple of nonlinear equations

$$\begin{aligned}
x_{\mu l} &= \tanh \left[\sum_{\nu \in A_1^{\text{col}}(l) \setminus \mu} \tanh^{-1} \hat{x}_{\nu l} + F \right], \\
y_{\mu l} &= \tanh \left[\sum_{\nu \in A_2^{\text{col}}(l) \setminus \mu} \tanh^{-1} \hat{y}_{\nu l} + \sum_{\nu \in A_3^{\text{col}}(l)} \tanh^{-1} \hat{z}_{\nu l} + F \right], \\
z_{\mu l} &= \tanh \left[\sum_{\nu \in A_2^{\text{col}}(l)} \tanh^{-1} \hat{y}_{\nu l} + \sum_{\nu \in A_3^{\text{col}}(l) \setminus \mu} \tanh^{-1} \hat{z}_{\nu l} + F \right], \\
\hat{x}_{\mu l} &= \text{sign}(J_{\mu}) \prod_{i \in A_1^{\text{row}}(\mu) \setminus l} x_{\mu i} \prod_{j \in A_2^{\text{row}}(\mu)} y_{\mu j}, \\
\hat{y}_{\mu l} &= \text{sign}(J_{\mu}) \prod_{i \in A_1^{\text{row}}(\mu)} x_{\mu i} \prod_{j \in A_2^{\text{row}}(\mu) \setminus l} y_{\mu j}, \\
\hat{z}_{\mu l} &= \text{sign}(J_{\mu}) \prod_{j \in A_3^{\text{row}}(\mu) \setminus l} z_{\mu j}
\end{aligned} \tag{17}$$

where $A^{\text{row}}(\mu)$ and $A^{\text{col}}(l)$ denote the sets of non-zero elements in the μ -th row and l -th column of matrix A , respectively.

Eqs.(17) can be solved iteratively from appropriate initial conditions (prior means are usually chosen as initial states). Less than 50 iterations are typically sufficient

for convergence. After obtaining the solutions, approximated posterior means can be calculated

$$\begin{aligned}\langle s_i \rangle &= \tanh \left[\sum_{\nu \in A_1^{\text{col}}(i)} \tanh^{-1} \hat{x}_{\nu i} + F \right], \\ \langle \sigma_j \rangle &= \tanh \left[\sum_{\nu \in A_2^{\text{col}}(j)} \tanh^{-1} \hat{y}_{\nu j} + \sum_{\nu \in A_3^{\text{col}}(j)} \tanh^{-1} \hat{z}_{\nu j} + F \right],\end{aligned}\quad (18)$$

which provides the MPM estimators $\hat{s}_i = \text{sign}(\langle s_i \rangle)$ and $\hat{\sigma}_j = \text{sign}(\langle \sigma_j \rangle)$.

It can be shown that the BP/TAP framework provides an exact result when the global structure of the connectivities is graphically expressed by a tree [14]. Unfortunately, it is still unclear how good are the approximations obtained when a given system does not admit a tree architecture.

The graphical architecture of LDPC codes generally has many loops, which implies the BP/TAP framework does not necessarily offer a good approximation. However, it is conjectured, and partially confirmed, that a nearly exact result can be obtained, as long as no other locally stable solutions exists, when the parity check matrix A is randomly constructed and in the limit $N \rightarrow \infty$; this is due to the fact that the typical loop length scales as $O(\ln N)$ for randomly constructed matrices, which implies that LDPC codes can be locally treated as trees ignoring the effect of loops [24].

Neglecting the effect of loops naturally leads to a macroscopic description of the BP/TAP algorithm (17) utilizing density functions of messages $x_{\mu l}$, $y_{\mu l}$, $z_{\mu l}$, $\hat{x}_{\mu l}$, $\hat{y}_{\mu l}$ and $\hat{z}_{\mu l}$, which becomes identical to the simple iteration of the saddle point equation (12) [24]. Surprisingly, the celebrated method known as the *density evolution* (DE) [13], recently discovered independently in the information theory community, reduces exactly to the same equation (12). As both of DE and the current analysis reduce to an identical equation (12), the estimates provided by the two frameworks generally coincide for the practical performance. However, as the concept of free energy is missing from the DE framework, it does not provide a way for evaluating the optimal performance, for a given code; this is naturally characterised, in the statistical physics framework by thermodynamical transitions between decoding success and failure phases.

V. RESULTS

In order to theoretically examine the typical performance that can be obtained by the linearly combined coding scheme, we solved the saddle point equations (12). Since solving the equations analytically is generally difficult, we mainly resorted to numerical methods. The solutions were obtained by iterating the saddle point equations (12), and approximating the distributions by

$O(10^4)$ sample vectors. Less than 50 iterations were typically sufficient for obtaining a solution.

Solving the equations for several parameter sets, assuming $\alpha > R_2/(R_1 + R_2)$, we found that the solutions can be classified into three categories depending on whether overlaps $M_{\mathbf{u}}$ and $M_{\mathbf{d}}$ are 1 or not. The first one is referred to the *ferromagnetic* (F) solution ($M_{\mathbf{u}} = M_{\mathbf{d}} = 1$) corresponding to perfect retrieval for both messages \mathcal{W}_1 and \mathcal{W}_2 . The *half-ferromagnetic* (HF) solution which is characterized by $M_{\mathbf{u}} \neq 1$ and $M_{\mathbf{d}} = 1$ implies that only the second message \mathcal{W}_2 is perfectly retrieved, while \mathcal{W}_1 is not. The last category, termed paramagnetic (P) solution, describes a decoding failure for both messages being characterized by $M_{\mathbf{u}} \neq 1, M_{\mathbf{d}} \neq 1$. The ferromagnetic solution always exists and is locally stable for $C_1 \geq 3$ and $C_3 \geq 3$, while one can find other solutions only for relatively higher noise levels. As the noise level increases, HF and P solutions emerge in this order.

The HF solution may look counter-intuitive because the corruption process for the second receiver is expressed as Eq. (1), which seems as if the codeword were transmitted to the second receiver in a relay scheme via the first receiver and, therefore, retrieval of \mathcal{W}_2 would fail unless \mathcal{W}_1 were correctly decoded. However, we must emphasize here the following two points. Firstly, HF does not imply that the first receiver fails in knowing \mathcal{W}_1 while the second receiver correctly retrieves \mathcal{W}_2 but means only \mathcal{W}_2 can be retrieved from the corrupted codeword by a single receiver given a corruption rate p . Therefore, even if the situation of the second receiver is provided by HF, the first receiver can retrieve \mathcal{W}_1 if his/her corruption rate is so low that the situation corresponds to F. Secondly, it should be noticed that the current code based on an upper triangular parity check matrix is designed to provide a higher error correction ability for \mathcal{W}_2 as it has to be transmitted to a farther place and relatively more resource is assigned for \mathcal{W}_2 in construction of a codeword \mathcal{X} for $\alpha > R_2/(R_1 + R_2)$, which makes it possible to produce the non-trivial solution HF. Therefore, for $\alpha < R_2/(R_1 + R_2)$, on other hand, we found only two solutions: F and P, and HF does not exist as the assignment of the resource for \mathcal{W}_2 in \mathcal{X} is not sufficient in this parameter region (Fig. 2).

The solution that has the lowest free energy among the three becomes thermodynamically dominant. As the noise level p becomes higher (or the field F becomes weaker), the dominant state changes from F to HF and P in this order. Since receivers are required to retrieve only their own messages, the transition point between HF and P corresponds to the maximum noise level for error free communication in the second channel while maximum noise level for the first channel is given by the transition point between F and HF.

However, this does not imply a successful decoding up to the critical points in *practical* time scales. Practical perfect decoding by the BP/TAP algorithm is possible only when no suboptimal solutions exist, which means

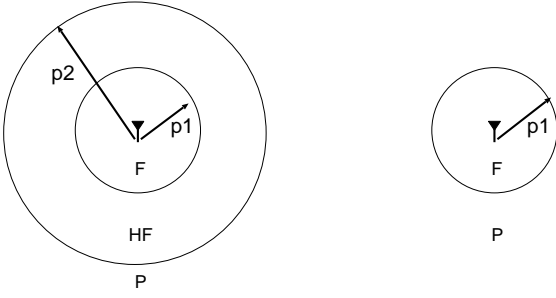


FIG. 2: Areas expressed by F, HF and P for a wireless degraded channel assuming that the noise corruption rate grows proportional to a distance from a sender (broadcast station). For $\alpha > R_2/(R_1 + R_2)$ (left), the area where \mathcal{W}_2 can be perfectly retrieved becomes larger than for $\alpha < R_2/(R_1 + R_2)$ (right) because of the existence of the HF solution.

that the practically achievable limit is given by the *spinodal points* of the HF and P solutions for the first and the second channels respectively; i.e., the point where new suboptimal solutions emerge. A similar phenomena has been reported before for similar systems [10, 11].

Fig.3 shows the maximum noise levels for perfect decoding of the linearly combined coding method obtained for $C_2 = 4$ and 0 fixing $C_1 = C_3 = 3$; $C_2 = 0$ corresponds to the sharing scheme for which $A_2 = 0$. One can find that both optimal and practical performances of the MPM decoder are improved by the introduction of the additional submatrix A_2 , as anticipated, in spite of the fact that the parameter $C_2 (= 4)$ is not optimally tuned. This result may induce the hope that Cover's limit can be saturated by optimally tuning the submatrices.

However, our analysis contradicts this conjecture. Solving Eq.(12) in the limit $C_3 \rightarrow \infty$ and C_1 or $C_2 \rightarrow \infty$ is feasible; it is known that the MPM decoder provides the optimal performance in this limit while practical BP/TAP decoding becomes difficult. The three solutions correspond to those already mentioned before, but can be analytically expressed as:

- *F solution:* Both messages are decodable ($M_{\mathbf{u}} = M_{\mathbf{d}} = 1$). The corresponding solutions and free energy are

$$\begin{cases} \pi(x) = \delta(x-1) \\ \rho(y) = \delta(y-1) \\ \phi(z) = \delta(z-1) \end{cases} \quad \begin{cases} \hat{\pi}(\hat{x}) = \delta(\hat{x}-1) \\ \hat{\rho}(\hat{y}) = \delta(\hat{y}-1) \\ \hat{\phi}(\hat{z}) = \delta(\hat{z}-1) \end{cases} \quad (19)$$

$$\mathcal{F} = -(1-2p)F.$$

- *HF solution:* Message \mathcal{W}_2 is only decodable ($M_{\mathbf{u}} \neq 1, M_{\mathbf{d}} = 1$).

$$\begin{cases} \pi(x) = \langle \delta(x - \tanh \xi F) \rangle_{\xi} \\ \rho(y) = \delta(y-1) \\ \phi(z) = \delta(z-1) \end{cases} \quad \begin{cases} \hat{\pi}(\hat{x}) = \delta(\hat{x}) \\ \hat{\rho}(\hat{y}) = \delta(\hat{y}) \\ \hat{\phi}(\hat{z}) = \delta(\hat{z}-1) \end{cases} \quad (20)$$

$$\mathcal{F} = (1 - \alpha - R_1) \ln 2 - (1 - 2p)F - (1 - \alpha) \ln 2H_2(p).$$

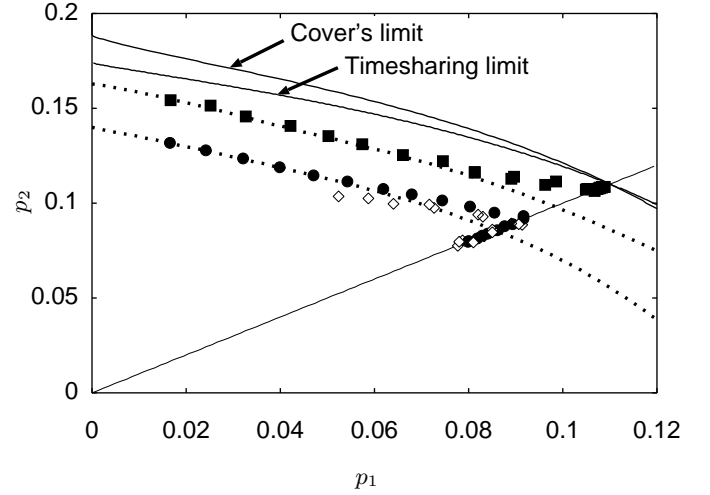


FIG. 3: Optimal and practical performance of the MPM decoder calculated by methods of statistical mechanics for different α values. For the first channel, the optimal performance is given by the thermodynamical transition between F and HF solutions while the transition between HF and P solutions marks the optimal performance for the second channel. On the other hand, the practical performance is given by the spinodal points of the HF and P solutions for the first and the second channels, respectively. Monte Carlo solutions based on 10^4 sample vectors were employed for solving the saddle-point equation (12). The standard deviation values resulting from 10 trials are smaller than the symbol size. The black squares and the black circles denote the optimal and the practical performances for the linearly combined coding scheme, where code parameters are set to $C_1 = C_3 = 3, C_2 = 4, R_1 = R_2 = 1/4$. Diamond symbols denote the maximum noise levels for decoding success by the BP/TAP algorithm, determined from 50 experiments. The error bars are smaller than the symbols. Broken lines denote the optimal and practical performances of the timesharing for corresponding LDPC codes. The two lines in the upper right are Cover's and timesharing capacities calculated in the information theory.

- *P solution:* Both messages are not decodable ($M_{\mathbf{u}} \neq 1, M_{\mathbf{d}} \neq 1$).

$$\begin{cases} \pi(x) = \langle \delta(x - \tanh \xi F) \rangle_{\xi} \\ \rho(y) = \langle \delta(y - \tanh \xi F) \rangle_{\xi} \\ \phi(z) = \langle \delta(z - \tanh \xi F) \rangle_{\xi} \end{cases} \quad \begin{cases} \hat{\pi}(\hat{x}) = \delta(\hat{x}) \\ \hat{\rho}(\hat{y}) = \delta(\hat{y}) \\ \hat{\phi}(\hat{z}) = \delta(\hat{z}) \end{cases} \quad (21)$$

$$\mathcal{F} = (1 - R_1 - R_2) \ln 2 - (1 - 2p)F - \ln 2H_2(p).$$

Examining the critical condition for decoding success in each channel, and comparing the free energy of the solutions, one obtains the capacity region of the linearly combined coding scheme

$$\begin{cases} R_2 < \alpha[1 - H(p_2)] \\ R_1 < (1 - \alpha)[1 - H(p_1)] \end{cases} \quad (22)$$

This is, unfortunately, identical to the timesharing capacity which can be achieved by a simple concatenation

of two independent codes. This result implies that the advantage of the linearly combined coding scheme vanishes as the submatrices become dense and this method cannot saturate Cover's limit.

VI. SUMMARY AND CONCLUSION

In this paper, we have examined the performance of linearly combined LDPC codes, for information transmission in a broadcast channel. Our analysis shows that the capacity of the suggested coding scheme is upper-bounded by the timesharing capacity, in spite of the apparent improvement in both optimal and practical performance with respect to LDPC based timesharing codes characterized by finite connectivity values.

The reason for the failure of linearly combined LDPC codes to saturate Cover's limit may be explained by the codeword structure produced by this scheme. In his proof, Cover optimized the code performance by introducing a specific structure termed the *cloud coding*, employing an auxiliary random variable \mathcal{U} as in Eq.(2). In cloud coding, a codeword \mathcal{X} is randomly generated according to $P(\mathcal{X}|\mathcal{U})$ around a *cloud center* \mathcal{U} sampled from $P(\mathcal{U})$. Knowing this structure, one can use the cloud center \mathcal{U} and the coset $\mathcal{X}_c = \mathcal{X} - \mathcal{U}$ for encoding \mathcal{W}_2 and \mathcal{W}_1 , respectively.

In the case of binary symmetric channels, the optimal cloud center \mathcal{U} can be obtained by sampling N bit unbiased vectors for which the entropy per bit can be maximized to 1. On the other hand, one can produce the optimal coset \mathcal{X}_c by independently and randomly generating each bit using a uniform bias $0 < \delta < 1$, which provides an entropy $H_2(\delta)$ per bit.

In an ideal situation, a noise vector ξ_1 which is biased with a flip probability p_1 is added to the coset \mathcal{X}_c in the first channel. This implies that the entropy of the received coset becomes $H_2(\delta * p_1)$ per bit while the entropy of the noise vector is $H_2(p_1)$ per bit. Since one can use the difference between the entropies to convey the information of \mathcal{W}_1 , the capacity of the first channel becomes $R_1 < H_2(\delta * p_1) - H_2(p_1)$, which is the second inequality of Eq.(2). On the other hand, for the second channel, characterized by a flip rate p_2 , the coset \mathcal{X}_c together with

a channel noise ξ_2 serves as a single noise vector for which the entropy becomes $H_2(\delta * p_2)$ per bit. As the entropy of the received cloud center can be maximized to 1 per bit, this means that the capacity of the second channel is given by $R_2 < 1 - H_2(\delta * p_2)$, which is the first inequality of Eq.(2).

In linearly combined coding scheme $(\begin{smallmatrix} G_1^T \\ G_3^T \end{smallmatrix})\mathcal{W}_2 + (\begin{smallmatrix} G_1^T \\ G_3^T \end{smallmatrix})\mathcal{W}_1$, $(\begin{smallmatrix} G_2^T \\ G_3^T \end{smallmatrix})\mathcal{W}_2$ becomes almost random, which may serve as the optimal cloud center. However, the second part $(\begin{smallmatrix} G_1^T \\ G_3^T \end{smallmatrix})\mathcal{W}_1$, that corresponds to the coset, is somewhat structured, differing from the optimal choice of uniformly biased random vectors.

In order to compare the structured coset with the optimal one, let us fix the maximum entropy per bit of $(\begin{smallmatrix} G_1^T \\ G_3^T \end{smallmatrix})\mathcal{W}_1$, which equals $1 - \alpha$, to that of the optimal coset $H_2(\delta)$. Then, one can show that the entropy of the corrupted coset with flip probability p per bit always increases from $H_2(p * \delta)$ to $(1 - \alpha) + \alpha H_2(p) = H_2(\delta) + H_2(p) \geq H_2(p * \delta)$. This means that the critical rate of the first channel increases from $H_2(\delta * p_1) - H_2(p_1)$ to $(1 - \alpha)[1 - H_2(p_1)]$ while that of the second channel reduces from $1 - H_2(p_2)$ to $\alpha[1 - H_2(p_2)]$. This trade-off between the capacities of the two channels limits the performance of linearly combined coding scheme to the timesharing limit, that is always within Cover's capacity region.

In conclusion, while the suggested linearly combined LDPC coding scheme provides an improved performance over LDPC based timesharing codes for finite connectivity constructions, in both theoretical and practical limits, it cannot go beyond the theoretical timesharing limit; for that to happen, different coding schemes should be examined.

Acknowledgments

Support by Grants-in-aid, MEXT (13680400 and 13780208) and JSPS (YK), The Royal Society and EPSRC-GR/N63178 (DS) is acknowledged.

-
- [1] T.M. Cover, IEEE Trans. Inform. Theory, **18**, 2 (1972).
 - [2] P.P. Bergmans, IEEE Trans. Inform. Theory, **19**, 197 (1973).
 - [3] T.M. Cover and J.A. Thomas, *Elements of Information theory* (Wiley, New York, 1991).
 - [4] T.M. Cover, IEEE Trans. Inform. Theory, **44**, 2524 (1998).
 - [5] R.G. Gallager, IRE Trans. Inform. Theory, **8**, 21 (1962).
 - [6] D.J.C. MacKay and R.M. Neal, *Lecture Notes in Computer Science* (Springer, Berlin, 1995), Vol. 1025, p.100
 - [7] M.C. Davey, *Record-breaking error correction using low-*

density parity-check codes, Hamilton prize essay, Gonville and Caius College, Cambridge (1998).

- [8] F.J. MacWilliams and N.J.A. Sloane, *The Theory of Error-Correcting Codes* (Amsterdam, North Holland, 1978).
- [9] W. Van Gils, IEEE Trans. Inform. Theory, **29**, 866 (1983); **30**, 544 (1984).
- [10] Y. Kabashima, T. Murayama and D. Saad, Phys. Rev. Lett. **84**, 1355 (2000).
- [11] Y. Kabashima, T. Murayama, D. Saad and R. Vicente, in *Advances in Neural Information Processing System*, **12**

- edited by S. Solla, T. Leen and K. Müller, (MIT Press, Cambridge, MA, 2000), p. 272
- [12] N. Surlas, *Nature*, **339**, 693 (1989).
 - [13] T. Richardson and R. Urbanke, *IEEE Trans. Inform. Theory*, **47**, 599 (2001).
 - [14] J. Pearl, *Probabilistic Reasoning in Intelligent Systems: Network of Plausible Inference* (San Francisco, CA: Morgan Kaufmann, 1988).
 - [15] H.A. Bethe, *Proc. R. Soc. London, Ser A* **151**, 552 (1935).
 - [16] J.S. Yedidia, W.T. Freeman and Y. Weiss, in *Advances in Neural Information Processing Systems*, **13**, edited by T.K. Leen, T. Dietterich and V. Tresp, (MIT press, Cambridge MA, 689 (2001).
 - [17] D.J. Thouless, P.W. Anderson and R.G. Palmer, *Phill. Mag.*, **35**, 593 (1977).
 - [18] Y. Kabashima and D. Saad, *Europhys. Lett.*, **44**, 668 (1998).
 - [19] Y. Kabashima, cond-mat/0211500 (2002).
 - [20] M. Mézard, G. Parisi and M.A. Virasoro, *Spin Glass Theory and Beyond* (World Scientific, 1987).
 - [21] H. Nishimori, *Statistical Physics of Spin Glasses and Information Processing* (Oxford University Press, Oxford, UK, 2001).
 - [22] H. Nishimori and D. Sherrington, *Disorderd and Complex Systems*, edited by P. Sollich, A.C.C. Coolen, L.P. Hughston and R.F. Streater (American Institute of Physics, New York, 2001), p.67
 - [23] Y. Iba, *J.Phys.A*, **32**, 3875 (1999).
 - [24] R. Vicente, D. Saad and Y. Kabashima, in *Advances in Neural Information Processing Systems*, **13**, edited by T.K. Leen, T. Dietterich and V. Tresp, (MIT press, Cambridge MA), 322 (2001).